IGARSS 2022 - 2022 IEEE International Geoscience and Remote Sensing Symposium | 978-1-6654-2792-0/22/$31.00 ©2022 IEEE | DOI: 10.1109/IGARSS46834.2022.9884607

ASSESSING THE PRISMA POTENTIAL FOR MINERAL EXPLORATION TO VECTOR LOW-GRADE LITHIUM DEPOSITS

Joana Cardoso-Fernandes[1,2], Douglas Santos[1], Alexandre Lima[1,2], Ana Cláudia Teodoro[1,2]

[1]Department of Geosciences, Environment and Spatial Planning, University of Porto, Porto, Portugal
[2]Institute of Earth Sciences (ICT), Porto, Portugal
*joana.fernandes@fc.up.pt

ABSTRACT

PRISMA data is still underexploited in what concerns mineral exploration, while the high demand for battery components such as lithium (Li) instigates exploration of other low-grade deposits such as St. Austell (Cornwall, UK). This study assesses the potential of PRISMA data to target such Li deposits through the detection of topaz as a proxy to the mineralization using band math and partial unmixing techniques. The topaz distribution maps obtained are coherent between each other and with the known geology of the area, highlighting the PRISMA potential, although there could be some shortcomings related to its spatial resolution. Comparison with Sentinel-2 or Worldview-3 data shows the limitations of multispectral products, despite some potential to use Worldview-3 that need to be further investigated. In the future, new approaches to directly detect Li-micas and field validation of the results must be conducted.

Index Terms— Band ratio, absorption band-depth, MTMF, topaz, hyperspectral

1. INTRODUCTION

With the launch of the PRecursore IperSpettrale della Missione Applicativa (PRISMA) hyperspectral satellite in 2019 by the Italian Space Agency, new possibilities for satellite-based approaches have emerged. Most studies assess the potential of PRISMA data in several applications, such as: (i) agriculture [1]; (ii) wildfires [2]; and (iii) hazard management [3]. There are also a few studies concerning lithological or mineral mapping [4, 5], but there is a need for more detailed approaches regarding mineral exploration.

Due to the current decarbonization and need to store renewable energy, there is an increased demand for battery components such as lithium (Li). Remote sensing has been employed to target Li pegmatite and brine deposits [6, 7], however, to meet the global demand it is also necessary to consider the exploration of low-grade Li deposits such as the St. Austell greisen deposit in Cornwall, UK [8]. The St. Austell region has been mainly exploited for China Clay, but previous airborne hyperspectral surveys allowed to identify lepidolite and topaz associated with the primary granite [9], making it the ideal study area to evaluate the PRISMA potential to detect such low-grade Li deposits. For this, real PRISMA data were confronted with available reference spectra from the United States Geological Survey (USGS) spectral library [10] and the results were compared with available multispectral data (Sentinel-2 and Worldview-3).

2. STUDY AREA

The study area is marked by several pits, spoil heaps, and mica lagoons (Fig. 1) from the China Clay exploitation, being kaoline a weathering product of the late-Variscan St. Austell granite [9, 11]. Distinct facies were identified in the St. Austell pluton, including: (i) biotite, (ii) Li-mica, (iii) tourmaline, (iv) topaz granites [11]. The topaz granite also contains Li-mica (varying from zinnwaldite to lepidolite) [9, 11]. Greisen Li deposits have formed by high-temperature hydrothermal alteration of the St. Austell granite [8].

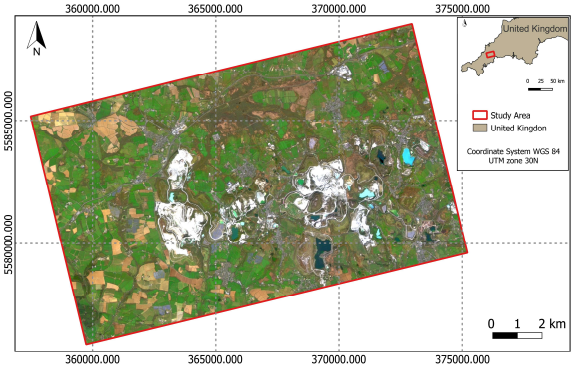

Fig. 1. PRISMA true color composite (5 m GSD) showing the location of the pits, spoil heaps, and lagoons of St. Austell.

3. DATA AND METHODS

3.1. Data

The PRISMA pushbroom sensor records 238 hyperspectral bands in the 400-2500 nm wavelength region (Fig. 2) with a 30 m ground-sampling distance (GSD) and a Panchromatic (PAN) band with 5 m GSD [5, 12]. An L2D level product collected on 05/04/2020 at 11:29 am, with cloud coverage of

3,27%, covering St. Austell was downloaded from the PRISMA Mission Catalog website (https://prisma.asi.it/). The product was provided at surface reflectance in the HDF-EOS5 (Hierarchical Data Format - Earth Observing System) file [12]. This file was converted into BSQ (band sequential) file format using ENVI 5.6.1 and the EnMap-Box plugin for QGIS before processing. A Color Normalized (Brovey) Sharpening was performed to obtain a true color composite with 5 m GSD (Fig. 1). To compare with the PRISMA data, a Sentinel-2 image acquired in 09/04/2020 and with processing level 2A was also downloaded from Copernicus open access Hub (https://scihub.copernicus.eu/). The Sentinel-2 Multispectral Instrument (MSI) has 13 spectral bands: 10 bands in the visible and near-infrared (VNIR) region and three on shortwave infrared (SWIR) [13]. Level 2A is provided at Surface reflectance, and no atmospheric correction was necessary.

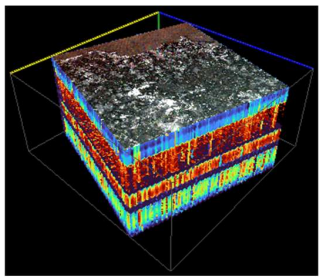

Fig. 2. PRISMA L2D data cube image, where each pixel corresponds to whole spectrum.

3.2. Methods

In this study, topaz was chosen as the target mineral due to its exclusive diagnostic absorption feature at 2080 nm (Fig. 3) [10]. Therefore, there should be no spectral confusion with other minerals, and since this absorption feature persists in mineral mixtures, topaz can work as a proxy to Li-rich granites. Topaz VNIR-SWIR spectra from the USGS spectral library [10] were resampled to PRISMA resolution using a Python library called SpectRes (Fig. 3). The USGS spectral library also provides the topaz spectra already resampled to several satellite sensors such as Worldview-3 and Sentinel-2 (Fig. 3). After resampling, two different approaches were used to map topaz. In addition, vegetation and water masks were computed for each satellite product.

3.2.1. Band calculations

Band ratio (BR) and relative absorption band-depth (RBD) were applied to PRISMA to target topaz based on its 2080 nm diagnostic absorption. While with BR one of the shoulders is divided by the absorption band, RBD divides the sum of one or several bands located on each of the shoulders by the sum of one or more bands located on the center of the absorption [14]. To determine the bands to be used in each method, the topaz spectral curves resampled to PRISMA resolution were analyzed (Fig. 3), being bands 173, 174, 175 on the left shoulder, bands 178 and 179 on the absorption center, and bands 182, 183, 184 on the right shoulder. Using QGIS version 3.22.1 raster calculator, six BR and five RBD were tested with the best results displayed in Chapter 4.

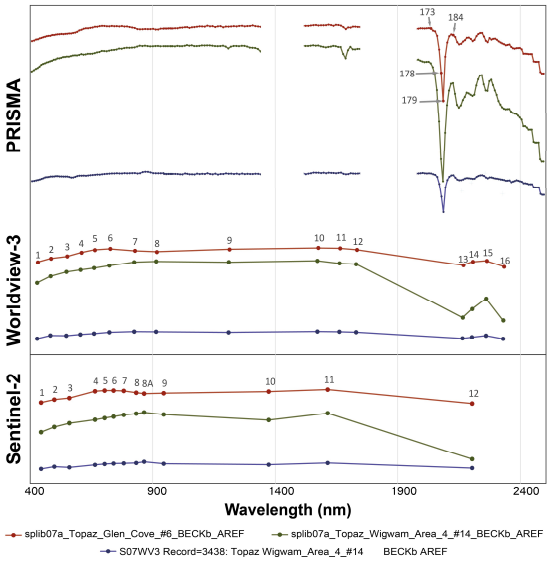

Fig. 3. Selected USGS topaz spectra resampled to Sentinel-2 and Worldview-3 [10], and PRISMA resolution (this study).

3.2.2. Mixture Tuned Matched Filtering (MTMF)

Mixture Tuned Matched Filtering (MTMF) is a method employed to find the abundance of user-defined endmembers and requires a Minimum Noise Fraction (MNF) transform of the data [9], both performed in ENVI 5.6.1. The MNF Rotation was applied to all 234 bands of PRISMA BSQ imagery and the sixteen MNF bands with less noise were selected as input files for the MTMF transform. The endmembers used were the pure topaz spectra from USGS spectral library. Preliminarily, MTMF outputs for each pixel a set of rule images, the Matched Filtering (MF) and the infeasibility scores, against each endmember spectrum [15]. This result was then used to classify the whole image, generating a raster with the pixels identified as topaz.

4. RESULTS AND DISCUSSION

As observed in Fig. 3, the 2080 nm absorption feature is clearly marked in band 179 (central wavelength at 2086.1 nm). In the case of Sentinel-2, the 2080 nm absorption feature is only noticeable in band 12 (center wavelength at 2203.4 nm) when the absorption is well pronounced, but, even so, band 12 is expected to be highly influenced by minerals with absorptions around 2220 nm and 2300 nm. Due to its higher spectral resolution, Worldview-3 has greater sensibility than Sentinel-2 but the 2080 nm absorption is only visible in band 13 (center wavelength at 2164.2 nm) when the absorption

strength is high (Fig. 3), reinforcing the relevance of PRISMA data for this type of application.

In what concerns the image processing methods, both BR, RBD and MTMF map topaz in an old pit northwest of the Nanpean village (purple rectangle of Fig. 4-a and -b), showing coherence between different methods. This area is located where topaz granite (also containing Li-micas) is mapped [9], thus corroborating the efficacy of the approach. However, the performance of the band math methods can change according to the selected bands: for example, BRs that employed bands from the right shoulder as the numerator (e.g. 182/179, 183/179, 184/179) showed better performance than the ones that employed bands from the left shoulder (e.g. 173/179, 174/179, 175/179). Despite this, BRs wrongly classify topaz in the Blackpool pit, currently filled with water, showing the ineffectiveness of the water mask in this pit. Equally, not all RBDs were effective in topaz mapping. In fact, only RBD 2 ([(173+174)+(183+184)]/179) allowed to identify topaz in the same area highlighted by BR and MTMF. Oppositely, RBD 4 ([(173+174+175)+(182+183+184)]/179) identifies topaz in the spoil heaps related to the Rostowrack pit (west of the old Nanpean pit; over the mapped topaz granite) and in the spoil heaps near the Longstone pit (over the Li-mica granite but where should be no topaz). RBD 4 also had a larger number of false positives when compared with RBD 2, wrongly mapping topaz in built-up areas or agricultural fields. Both RBDs wrongly classified some water pixels as topaz in the Blackpool pit. Regarding the MTMF results, there are also some noteworthy false positives: (i) the Blackpool pit is entirely misclassified as topaz (Fig. 4); (ii) topaz is also identified in some of the other pits that are not locater over the topaz granite; and (iii) there are some pixels classified as topaz in the agricultural fields.

Lastly, the spectral response of the area identified as topaz-bearing in the purple rectangle of Fig. 4 was investigated in both PRISMA and Sentinel-2 images, and the spectral curves were compared using the EnMap-Box plugin (Fig. 5). As expected, Sentinel-2 band 12 is influenced by the AlOH absorption at ~2220 nm. However, in the PRISMA image, it was not possible to identify the diagnostic 2080 nm absorption of topaz. Since Fig. 3 demonstrates that PRISMA has enough spectral resolution, this could be a consequence of the 30 m GSD, resulting in spectral mixing at the pixel level.

5. CONCLUSIONS

This study evaluates the potential of PRISMA data for the exploration of low-grade Li deposits through the detection of topaz as a proxy mineral. Comparing the topaz reference spectra resampled to PRISMA, Worldview-3 and Sentinel-2, PRISMA is undoubtedly the best product to detect the topaz diagnostic feature at 2080 nm, although there could be some potential in using Worldview-3 images that needs to be verified in the future. Then two approaches were employed to map topaz distribution: (i) band math (BR and RBD), and (ii) partial unmixing (MTMF). The results obtained with the distinct techniques employed were consistent and coherent with the known location of the topaz granite, confirming the PRISMA adequacy for such approach, although field validation should be conducted. However, the proper choice of bands in BR and RDB was crucial to obtain good results. Also, MTMF showed a large number of topaz false positives when compared to BR. Nonetheless, the PRISMA 30 m GSD can be a major shortcoming, since it was not possible to identify topaz endmembers directly on the image pixels. Pansharpening techniques could be employed in the future to address this problem. Comparison with Sentinel-2 images confirmed the limitations of such multispectral products. New approaches can be employed to target the Li deposits of the area.

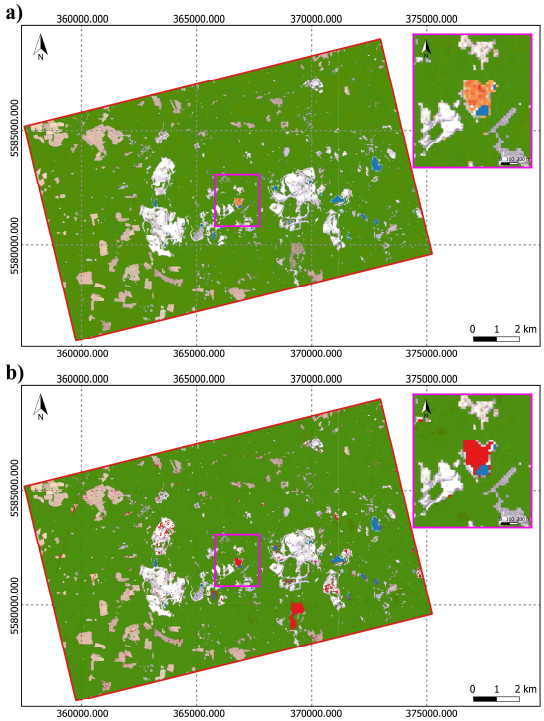

Fig. 4. High 182/179 ratio values in warm colors, where red pixels represent areas where topaz is expected to be present (**a**) and MTMF topaz classification in red pixels (**b**) over true color PRISMA image, with vegetation (green) and water (blue) masks.

6. ACKNOWLEDGEMENTS

This study is funded by FCT–Fundação para a Ciência e a Tecnologia, I.P., with the projects UIDB/04683/2020 and UIDP/04683/2020 - ICT (Institute of Earth Sciences), by Commission's Horizon 2020 innovation programme under grant agreement No 869274, GREENPEG project, and by ANI and COMPETE 2020 with POCI-01-0247-FEDER-046083, INOVMINERAL project.

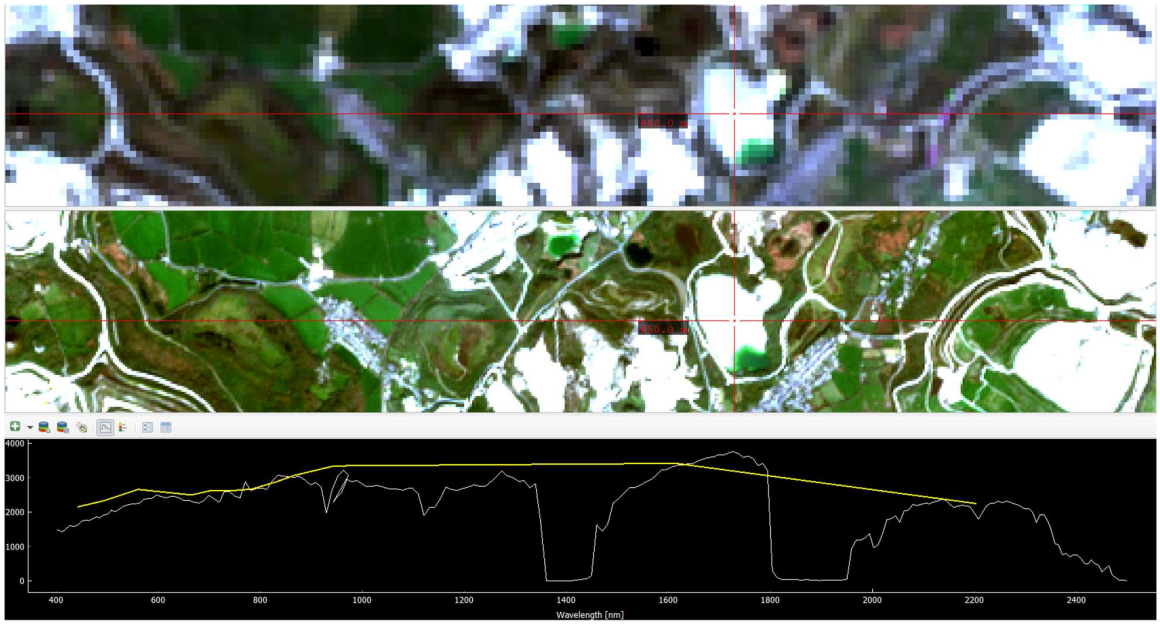

Fig. 5. Comparison of the spectral signature of the area highlight by the band ratios, RDB and MTMF for PRISMA (top; white spectrum) and Sentinel-2 (middle; yellow spectrum).

7. REFERENCES

[1] U. Amato *et al.*, "Statistical Classification for Assessing PRISMA Hyperspectral Potential for Agricultural Land Use," *IEEE Journal of Selected Topics in Applied Earth Observations and Remote Sensing,* vol. 6, no. 2, pp. 615-625, 2013.

[2] G. Lazzeri, W. Frodella, G. Rossi, and S. Moretti, "Multitemporal Mapping of Post-Fire Land Cover Using Multiplatform PRISMA Hyperspectral and Sentinel-UAV Multispectral Data: Insights from Case Studies in Portugal and Italy," *Sensors,* vol. 21, no. 12, p. 3982, 2021.

[3] R. De Bonis *et al.*, "The potential impact of the next hyperspectral prisma mission on the natural and anthropogenic hazards management," in *2015 IEEE 15th International Conference on Environment and Electrical Engineering (EEEIC)*, 2015, pp. 1643-1646.

[4] P. Tripathi and R. D. Garg, "Feature Extraction of DESIS and PRISMA Hyperspectral Remote Sensing Datasets for Geological Applications," *Int. Arch. Photogramm. Remote Sens. Spatial Inf. Sci.,* vol. XLIV-M-3-2021, pp. 169-173, 2021.

[5] D. Heller Pearlshtien, S. Pignatti, U. Greisman-Ran, and E. Ben-Dor, "PRISMA sensor evaluation: a case study of mineral mapping performance over Makhtesh Ramon, Israel," *International Journal of Remote Sensing,* vol. 42, no. 15, pp. 5882-5914, 2021/08/03 2021.

[6] J. Cardoso-Fernandes *et al.*, "Interpretation of the Reflectance Spectra of Lithium (Li) Minerals and Pegmatites: A Case Study for Mineralogical and Lithological Identification in the Fregeneda–Almendra Area," *Remote Sensing,* vol. 13, no. 18, p. 3688, 2021.

[7] J. Cardoso-Fernandes, A. C. Teodoro, and A. Lima, "Remote sensing data in lithium (Li) exploration: A new approach for the detection of Li-bearing pegmatites," *International Journal of Applied Earth Observation and Geoinformation,* vol. 76, pp. 10-25, 2019/04/01/ 2019.

[8] B. Gourcerol, E. Gloaguen, J. Melleton, J. Tuduri, and X. Galiegue, "Re-assessing the European lithium resource potential – A review of hard-rock resources and metallogeny," *Ore Geology Reviews,* vol. 109, pp. 494-519, 2019/06/01/ 2019.

[9] R. J. Ellis and P. W. Scott, "Evaluation of hyperspectral remote sensing as a means of environmental monitoring in the St. Austell China clay (kaolin) region, Cornwall, UK," *Remote Sensing of Environment,* vol. 93, no. 1, pp. 118-130, 2004/10/30/ 2004.

[10] R. F. Kokaly *et al.*, "USGS Spectral Library Version 7," in "Data Series," Reston, VA, Report 1035, 2017, Available: http://pubs.er.usgs.gov/publication/ds1035.

[11] D. A. C. Manning, P. I. Hill, and J. H. Howe, "Primary lithological variation in the kaolinized St Austell Granite, Cornwall, England," *Journal of the Geological Society,* vol. 153, no. 6, p. 827, 1996.

[12] R. Guarini *et al.*, "Prisma Hyperspectral Mission Products," in *IGARSS 2018 - 2018 IEEE International Geoscience and Remote Sensing Symposium*, 2018, pp. 179-182.

[13] European Space Agency (ESA). (January 2018). *User Guides: Sentinel-2 - Overview*. Available: https://sentinel.esa.int/web/sentinel/user-guides/sentinel-2-msi/overview

[14] J. K. Crowley, D. W. Brickey, and L. C. Rowan, "Airborne imaging spectrometer data of the Ruby Mountains, Montana: Mineral discrimination using relative absorption band-depth images," *Remote Sensing of Environment,* vol. 29, no. 2, pp. 121-134, 1989/08/01/ 1989.

[15] L3Harris. (2020, 5 January 2022). *Mixture Tuned Matched Filtering*. Available: https://www.l3harrisgeospatial.com/docs/mtmf.html